ACTA STEREOL 1999; 18/2: 247-254
ORIGINAL SCIENTIFIC PAPER

3D SPATIAL TIME STRUCTURE SIMULATIONS BY REACTION-DIFFUSION MODELS

Luc Decker, Dominique Jeulin

Centre de Morphologie Mathématique, Ecole des Mines de Paris
35, rue Saint-Honoré, F-77300 Fontainebleau, France

ABSTRACT

Classical reaction-diffusion models are studied with respect to their 3D aspects. Simulations based on the coupled map lattice method are considered as numerical experiments which allow one to investigate the genesis of complex random structures and their evolution in time. Results are mostly presented under the form of realistic rendering of binary structures by the application of a ray-tracing software. Specific properties of this class of structures are also pointed out.

Key words: random media, reaction-diffusion, simulations, 3D.

INTRODUCTION

When kept far from thermodynamic equilibrium, chemical systems coupled with diffusion show nonlinear behaviors and generate concentration patterns with a high organization level (Turing, 1952; Nicolis and Prigogine, 1977). Realistic textures, such as those encountered in natural phenomena (rocks, biological tissues,...) can be easily generated from these models and therefore the assumption was made that a reaction-diffusion mechanism is indeed at the origin of the observed patterns. However, there are very few data about their three-dimensional aspects in the literature, probably because of computational complexity (very small domains were used) and of obstacles to visualization. We give here an overview of well known reaction-diffusion models and present results of three-dimensional simulations.

REACTION-DIFFUSION EQUATIONS

On the macroscopic scale of a continuum, the evolution of an N-species reaction-diffusion model is ruled by the following general set of partial differential equations :

$$\frac{\partial Z_i(x,t)}{\partial t} = div(D_i(x)\ grad\ Z_i(x,t)) + F_i(Z_1, Z_2, ..., Z_N) \qquad (1)$$

where the studied variables $Z_i(x,t)$ are the space-time dependent chemical concentrations or densities of the different components. The $F_i(Z_1, ..., Z_N)$ term is a nonlinear function

which expresses the reaction part of the model. In the case of a real reaction scheme, the F_i function – usually polynomial – is obtained from the basic stoichiometric rules and involves the kinetic constants of the elementary reactions. When the diffusion coefficients D_i of the species are not space dependent, the diffusion term $div(D_i(x)\ grad\ Z_i(x,t))$ in Eq. 1 can be simplified to the more usual form $D_i \triangle Z_i(x,t)$. In the present case, we impose initial conditions which correspond to a set of critical concentrations with the addition of a small amount of uniform random noise. As a consequence, the $Z_i(x,t)$ variables are considered as *random functions*.

IMPLEMENTATION ASPECTS

Reaction-diffusion simulations can be viewed as an application of the coupled map lattice model (Kaneko, 1992). When dealing with large sets of 3D data (up to 15 billions voxels in the present case), an optimization of the basic reaction-diffusion computation step is really advisable. The processed domain consists in a set of N images of floating point numbers, usually with periodic boundary conditions. First, the diffusion part is carried out by an efficient discrete Laplacian algorithm using a $3 \times 3 \times 3$ convolution kernel filled by only two different weights ($1 - D_i$ for the center point and $D_i/26$ for all first and second neighbors). This algorithm runs "in situ" – the output results are stored into the same input domain – and takes the advantage of the structure of the cubic kernel to use a shifting window (the computation at point x is partly based on the computation at point $x - 1$). This diffusion operator was tested successfully by the study of the Gaussian dispersion of a punctual impulse, provided that $0.1 \leq D_i \leq 1$ to avoid numerical instabilities. By introducing second order neighbors in the kernel, one also avoids a parity (i.e. checkerboard) effect when $D_i \approx 1$, which results from the decomposition of the domain into interlaced independent sub-domains. The reaction part may be optimized more classically by detecting common expressions in the $F_i(Z_j)$ functions and by the factorization of terms. A parallel version (coarse grain type) of the simulation program was also written, based on the MPI standard, and was run on a IBM-SP2 architecture. The processed domain is simply shared in slices among several processors, whereas the communications consist only in the synchronous exchange of the sub-domain boundaries (2D images) at each iteration. With 8 processors, the measured performance decreases by about 17% in comparison with a sequential execution, and the computation overall speed reaches 700 MFLOPS, which corresponds to more than 14 billion voxels per second.

VISUALIZATION

The simulation of 3D reaction-diffusion structures requires adequate space-time visualization techniques. This point is crucial for a better understanding of the complex behavior of the models and of the observation of their particular morphology. In a first approach, any section of the processed domain may be simply converted into a false color 8-bit image for each species (scaling the concentration into a $0-255$ discrete range). In the same way, the sides of the computed domain can be mapped onto a 3D parallepipedic volume. However, reaction-diffusion patterns are also about to be transformed into binary sets by the selection of concentration ranges, since they usually consist in domains of homogeneous concentration. This step allows us to apply a ray-tracing software, namely Persistence of Vision (POV-Ray, 1996) to produce realistic renderings of the structures, using some given view point, illumination, texture, and projection parameters. Each voxel which

belongs to the surface of the binary set to be represented is simply added to the tracing instructions. Additional smoothing is computed by the rendering software, and is based on the contributions of radial fields centered in each voxel, namely a *blob* primitive. This kind of smoothing is well adapted to reaction-diffusion structures. Finally, the model evolution in time is taken into account either by the editing of video sequence (built from images generated every δt iterations), or by the creation of some spatiotemporal images, where one of the coordinates represents time and the other gives the concentration value along a selected profile of the domain.

SCHLÖGL MODEL

The Schlögl model (Schlögl, 1972) describes a quite simple three-species chemical scheme, based on four elementary reactions. One can reduce this system to a single species scheme, where the chemical reaction term is a polynomial of degree three in the concentration of the single species, leading to one unstable steady state $Z = a_0$ and to two stable states $Z = a_1$ and $Z = a_2$, with $a_1 < a_0 < a_2$. Actually the model follows the reaction-diffusion equation (RDE) :

$$\begin{array}{l} \frac{\partial Z(x,t)}{\partial t} = D \triangle Z + k_0 - k_1 Z + k_2 Z^2 - k_3 Z^3 \\ with \;\; k_0 = 0.002, \; k_1 = 0.0390, \; k_2 = 0.07125, \; k_3 = 0.030625 \end{array} \qquad (2)$$

Such a nonlinear dynamics is at the origin of an auto-catalytic behavior. When the system is initially set in the unstable state a_0 with the addition of random noise, a bifurcation occurs. At a macroscopic level, spatially organized parts of the domain fall over either one of the stable states, as shown in Fig. 1. These spherical type regions are growing, but it should be noticed that coalescence phenomena occur and modify the medium morphology. Finally, one state invades the whole domain. In two dimensions, similar random textures have already been simulated using a cellular automaton (Dab et al., 1990) or a lattice gas automaton (Decker and Jeulin, 1996).

TURING STRUCTURES

The class of reaction-diffusion models which are at the origin of Turing type structures (Turing, 1952) is by far the most studied and the larger one. It appears that at least a two-species chemical scheme is required to produce such complex structures, in relation with a nonlinear dynamics. In particular, when the diffusion coefficients of the two species are different enough, the chemical reactions generate some stationary concentration heterogeneities (i.e. coexistence of homogeneous domains with different concentrations), showing a macroscopic and semi-regular spatial organization. More precisely, one of the species involved acts as an activator with diffusion coefficient D_1, whereas the other component acts as an inhibitor with diffusion coefficient $D_2 \gg D_1$ and hinders the spreading of the slower activator by its chemical action. The resulting patterns show a very low evolution rate and are therefore considered to be quasi-stable. Depending on the model, but also on its parameters and the initial concentrations, Turing structures show various semi-regular geometries, like pseudo-periodic tessellations, or stripes (Borckmans et al., 1992). To illustrate this class of models, we review here different RDEs, and we propose at least one three-dimensional representative realization, using a given set of parameters.

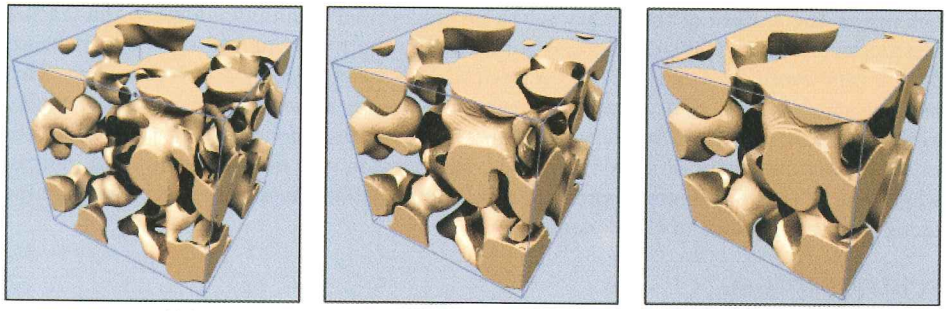

$t = 1000$ $t = 1500$ $t = 2000$

Fig. 1. Schlögl model: evolution with time. Binary structure: threshold $Z(x,t) > 1.45$. Initial conditions: $Z(x, t = 0) \approx 0.75556$. Domain size: $250 \times 250 \times 250$.

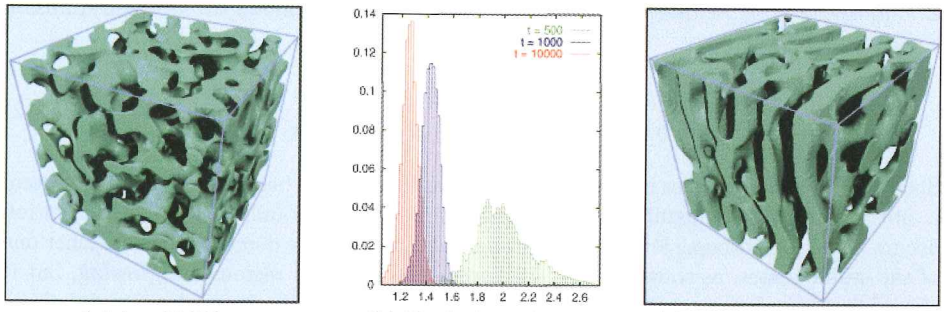

(a) $t = 10000$ (b) Evolution of the tortuosity distribution. (c) Anisotropic structures (diffusion with a drift).

Fig. 2. Turing structures: symmetrical model. $\alpha = 1.0$, $\beta = 1.0$, $D_2/D_1 = 3$. Binary structure: threshold $Z_1(x,t) > 2.20$. Initial conditions: $Z_i(x, t = 0) \approx 1.0$. Domain size: $200 \times 200 \times 200$.

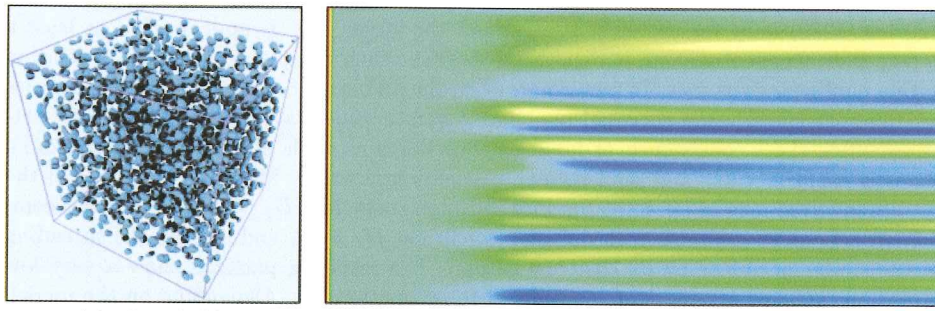

(a) Threshold: $Z_1(x, t = 50000) > 3.7$ (b) Spatio-temporal plot of $Z_1(x,t)$ (false colors). Time is running to the right, from $t = 0$ to $t = 42000$.

Fig. 3. Brusselator model. $\alpha = 2.3$, $\beta = 3.4$, $D_2/D_1 = 8.0$. Initial conditions: $Z_1(x, t = 0) \approx 4.5$, $Z_2(x, t = 0) \approx 1.5$. Domain size: $200 \times 200 \times 200$.

Symmetrical model. This system, studied by Walgraef (1988), offers a nice example of a Turing structure formation. It is based on the following RDE :

$$\begin{cases} \frac{\partial Z_1}{\partial t} = D_1 \triangle Z_1 + f(Z_1, Z_2) \\ \frac{\partial Z_2}{\partial t} = D_2 \triangle Z_2 - f(Z_1, Z_2) \\ f(Z_1, Z_2) = \beta\, Z_2\, {Z_1}^2 - \alpha\, Z_1 \end{cases} \quad (3)$$

Fig. 2a shows a binary structure resulting from a 3D simulation. We highlight the interesting property that this type of structure is fully interconnected (a unique connected component). Moreover, it appears that such a structure is well suited for modeling some kinds of porous media. Thus, as an example of advanced measurements, the tortuosity distribution (Decker et al., 1998) was estimated on the binary structure for the presented realization (Fig. 2b). In addition, anisotropic structures can be obtained by introducing a linear drift in the diffusion process, as shown in Fig. 2c. A similar extension of this model was proposed to simulate dislocations in metals (Walgraef et al., 1987).

Brusselator model (Prigogine and Lefever, 1968). This classical reaction-diffusion model is very close to the previous one. The equations involved are:

$$\begin{cases} \frac{\partial Z_1}{\partial t} = D_1 \triangle Z_1 + \alpha - (\beta + 1)\, Z_1 + {Z_1}^2\, Z_2 \\ \frac{\partial Z_2}{\partial t} = D_2 \triangle Z_2 + \beta\, Z_1 - {Z_1}^2\, Z_2 \end{cases} \quad (4)$$

Very regular structures can be obtained by the Brusselator, but with some randomly located defects or deviations. Fig. 3a gives an example of such structures in 3D, which can be compared with a random set based on the implantation of spherical primary grains with a repulsion distance (namely, a hard-core model). The spatiotemporal image presented in Fig. 3b gives the evolution of a profile of this realization.

Maginu model (Maginu, 1975). In two dimensions, this model is, in particular, at the origin of maze-like patterns, with a high tortuosity — in this case, a geodesic propagation algorithm is obviously very useful to look for a crossing path, i.e. to detect the possibility of percolation. The RDE takes the following form:

$$\begin{cases} \frac{\partial Z_1}{\partial t} = D_1 \triangle Z_1 + Z_1 - \frac{{Z_1}^3}{3} - Z_2 \\ \frac{\partial Z_2}{\partial t} = D_2 \triangle Z_2 + \frac{Z_1 - k\, Z_2}{c} \end{cases} \quad (5)$$

For a higher dimension, we also obtain such intricate structures, as shown in the realization presented in Fig. 4a, which looks like a very branched three dimensional network (the structure is totally interconnected). The distribution of the concentration Z_1 evolves principally during the genesis of the structure (at the beginning of the simulation), as shown in Fig. 4b.

COMPLEX GINZBURG-LANDAU EQUATION

This last model was selected to give an example of reaction-diffusion structures with a very different morphology. The complex time-dependent Ginzburg-Landau equation describes the evolution, following a Hopf bifurcation, of the slowly varying modulations in an extended system. Many numerical studies in one or two dimensions (see for instance Kuramoto, 1984) have been published about this famous model, which arises from

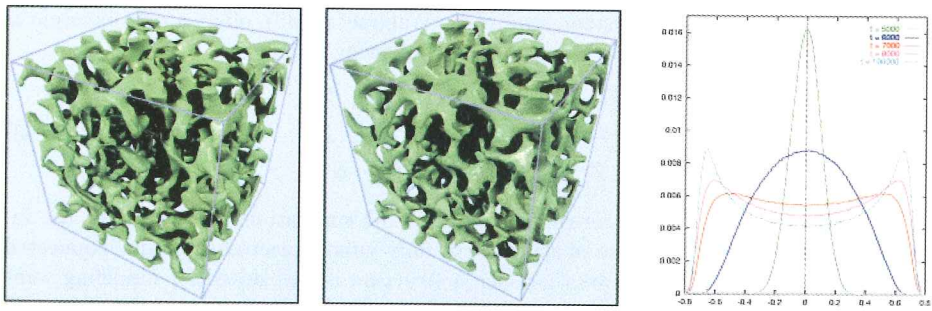

(a) $t = 10000$ $t = 100000$ (b) Evolution of $Z_1(x,t)$ distribution

Fig. 4. Maginu model. $k = 0.9$, $c = 0.45$, $D_2/D_1 = 6$. Binary structure: threshold $Z_1(x,t) > 0.60$. Initial conditions: $Z_i(x, t = 0) \approx 0.0$. Domain size: $200 \times 200 \times 200$.

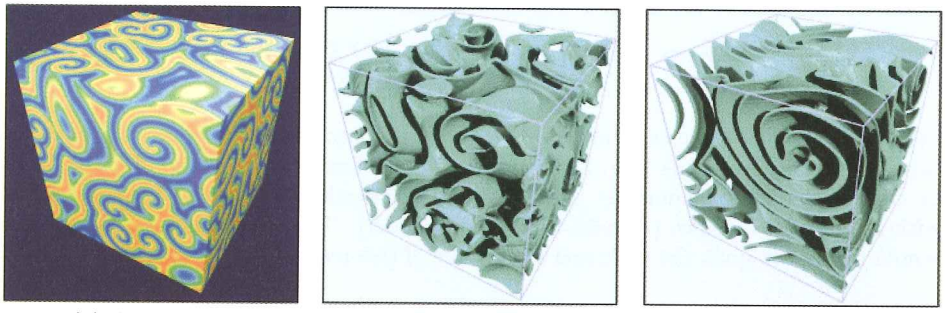

(a) Z_1, sides in false colors $t = 2000$ $t = 10000$ (b) Binary structure: threshold $Z_1(x,t) > 0.90$

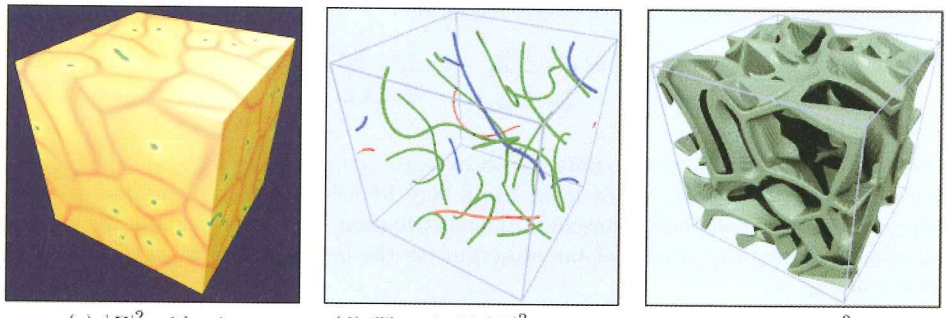

(c) $|Z|^2$, sides in false colors (d) Threshold $|Z|^2 < 0.18$, 3 connected components (e) Threshold $|Z|^2 > 0.93$

Fig. 5. Ginzburg-Landau model. $t = 2000$ (when not specified), $\alpha = 1$, $\beta = 1$, $\gamma = 1$, $\delta = 1.122$. Initial conditions: $Z_i(x, t = 0) \approx 0.0$. Domain size: $200 \times 200 \times 200$.

the analysis of numerous physical situations like hydrodynamic flows, nonlinear optics, or uncommon cases of chemical systems. This RDE can be viewed as a two-species scheme :

$$\frac{\partial Z}{\partial t} = D \triangle Z + A Z - B |Z|^2 Z$$
$$with \begin{cases} Z = Z_1 + i Z_2 \\ A = \alpha + i \gamma \\ B = \beta + i \delta \end{cases} \quad (6)$$

This equation admits spiral wave solutions, with oscillating and rotating behaviors. In Fig. 5a and 5b, resulting from a 3D simulation (starting with a white noise as initial conditions), one can clearly notice the presence of a population of spiral structures. Moreover, some other interesting features are also to be found in the image of the modulus $|Z|^2$ (Fig 5c). On the one hand, a low level threshold gives the minima of the modulus, which form worm-like structures (Fig. 5d), more precisely a population of interlocked tori. These minima correspond to the "axes" of the spiral structures. On the other hand, a high level threshold allows one to detect the boundaries of a population of cells (Fig. 5e), where one can verify that each cell contains a unique spiral structure. Actually the worm-like structures represent the skeleton of the cells, which are also of toric morphology. During their slow evolution, these cells interact, with attraction phenomena, and in some cases collapse (reducing progressively the number of cells). When a cell collapses, its volume is gradually filled by its neighboring cells, determining in this way zones of influence. The consequences of the periodic boundary conditions are still to be investigated.

CONCLUSION

From the 3D reaction-diffusion simulations, with a large range of morphologies, it is possible to generate interesting realizations of random media. Their morphological properties, still to be studied in details, can be directly measured in the three-dimensional space from the simulations. This will be of great help for practical applications of these models.

REFERENCES

Borckmans P, De Wit A, Dewel G. Competition in ramped Turing structures. Physica A 1992; **188**:137-157.

Dab D, Lawniczak A, Boon JP, Kapral R. Cellular-automaton model for reactive systems. Phys Rev Lett 1990; **64**:2462-2465.

Decker L, Jeulin D. Texture simulation by lattice gas from reaction-diffusion models. Microsc Microanal Microstruct 1996; **7**:565-571.

Decker L, Jeulin D, Tovena I. 3D morphological analysis of the connectivity of a porous medium. In the same volume, 1998.

Kaneko K. Overview of coupled map lattices. Chaos 1992; **2**(3):279-282.

Kuramoto Y. Chemical oscillations,waves,and turbulence. Berlin: Springer-Verlag, 1984.

Maginu K. Math Biosci 1975; **27**:17. J Differential Equations 1978; **31**:130.

Nicolis G, Prigogine I. Self-organization in nonequilibrium systems. New York: Wiley, 1977.

POV-Ray. Persistence of Vision (tm) ray-tracer software. User's documentation, 1996. See web site at *www.povray.org*.

Prigogine I, Lefever R. J Chem Phys 1968; **48**:1695.
Turing AM. The chemical basis of morphogenesis. Phil Trans Roy Soc London 1952; **B237**:37.
Schlögl F. Z Phys 1972; **253**:147-161.
Walgraef D, Schiller C, Aifantis EC. Reaction-diffusion approach to dislocation patterns. In: Walgraef D, ed. Patterns, defects and microstructures in nonequilibrium systems. Dordrecht: Martinus Nijhoff, 1987:257-269.
Walgraef D. Instabilities and patterns in reaction-diffusion dynamics. Solid State Phenomena 1988; **3-4**:77.

Presented at the 7th European Congress for Stereology, Amsterdam, April 20th to 23rd, 1998.